UAV-based canopy textures assess changes in forest structure from long-term degradation

Clément Bourgoin[1,2,3]*, Julie Betbeder[1,2,4], Pierre Couteron[5], Lilian Blanc[1,2], Hélène Dessard[1,2], Johan Oszwald[6], Renan Le Roux[1,2], Guillaume Cornu[1,2], Louis Reymondin[3], Lucas Mazzei[7], Plinio Sist[1,2], Peter Läderach[3] and Valéry Gond[1,2]

[1] CIRAD, Forêts et Sociétés, F-34398 Montpellier, France

[2] Forêts et Sociétés, Univ Montpellier, CIRAD, Montpellier, France.

[3] International Center for Tropical Agriculture (CIAT), Hanoi, Vietnam

[4] Ecosystems Modelling Unity, Forests, Biodiversity and Climate Change Program, Tropical Agricultural Research and Higher Education Center (CATIE), Turrialba, Cartago, Costa Rica

[5] UMR AMAP-IRD, Montpellier, France

[6] UMR CNRS LETG 6554, Laboratory of Geography and Remote Sensing COSTEL, Université de Rennes 2

[7] EMBRAPA Amazônia Oriental, Trav. Dr. Enéas Pinheiro, Bairro Marco, CEP, 66095-903 Belém, Pará, Brazil

* Correspondance: Clément Bourgoin, Campus International de Baillarguet, TA C-105/D 34398 Montpellier Cedex 5. E-mail : bourgoin.clement2@gmail.com

Abstract:

Degraded tropical forests dominate agricultural frontiers and their management is becoming an urgent priority. This calls for a better understanding of the different forest cover states and cost-efficient techniques to quantify the impact of degradation on forest structure. Canopy texture analyses based on Very High Spatial Resolution (VHSR) optical imagery provide proxies to assess forest structures but the mechanisms linking them with degradation have rarely been investigated. To address this gap, we used a lightweight Unmanned Aerial Vehicle (UAV) to map 739 ha of degraded forests and acquire both canopy VHSR images and height model. Thirty-three years of degradation history from Landsat archives allowed us to sample 40 plots in undisturbed, logged, over-logged and burned and regrowth forests in tropical forested landscapes (Paragominas, Pará, Brazil). Fourier (FOTO) and lacunarity textures were used to assess forest canopy structure and to build a typology linking degradation history and current states. Texture metrics capture canopy grain, heterogeneity and openness gradients and correlate with forest structure variability (R2= 0.58). Similar structures share common degradation history and can be discriminated on the basis of canopy texture alone (accuracy = 55%). Over-logging causes a lowering in forest height, which brings homogeneous textures and of finer grain. We identified the major changes in structures due to fire following logging which changes heterogeneous and intermediate grain into coarse textures. Our findings highlight the potential of canopy texture metrics to characterize degraded forests and thus be used as indicators for forest management and degradation mitigation. Inexpensive and agile UAV open promising perspectives at the interface between field inventory and satellite characterization of forest structure using texture metrics.

Highlights:

- We assessed canopy texture – structure relations along forest degradation gradients
- Canopy textures capture 58% of degradation-induced variability of canopy structure
- Degradation generates specific canopy textures linked with logging and fire history
- Texture metrics can be used to evaluate the state of degraded forests

Keywords: Canopy structure, Forest degradation, Remote Sensing, Texture, Tropical forest, Unmanned Aerial Vehicle.

1. Introduction

Forest degradation is a threat (Potapov et al., 2017) to the provision of ecosystem services by tropical forests. Degradation causes loss of biodiversity through habitat disturbance and fragmentation (Barlow et al., 2016; Broadbent et al., 2008), erosion of hydrological and soil properties, the reduction of non-timber forest resources (Lewis et al., 2015; Thompson et al., 2009), and currently accounts for 68.9% of overall carbon losses from tropical forests (Baccini et al., 2017).

The accumulation of forest disturbances such as selective logging and understory fires affects the states of the forest by destroying the canopy and the internal structure without triggering any changes in land use (Ghazoul and Chazdon, 2017; Putz and Redford, 2010). Degraded forests are therefore the consequence of complex degradation and recovery processes, which creates a gradient of varying structures within the forest landscape (Chazdon et al., 2016; Malhi et al., 2014).

Measuring the current forest structure and its degree of degradation are crucial for effective but sustainable management of degraded forests to guarantee the conservation, management and betterment of their ecological values (Goldstein, 2014).

However, the identification, characterization and measurement of forest degradation remains a scientific challenge, in particular in the remote sensing community (Frolking et al., 2009; Herold et al., 2011; Hirschmugl et al., 2017; Mitchell et al., 2017). Among the wide range of remote sensing approaches, optical time series of medium resolution Landsat images have been used to derive forest states indicators and to reconstruct forest degradation history through the detection and quantification of disturbances within the canopy (Asner et al., 2009; Bullock et al., 2018; DeVries et al., 2015; Souza et al., 2013). These approaches are steps towards degradation monitoring and informing Reducing Emissions from Deforestation and Degradation (REDD+) systems (Goetz et al., 2014) but do not provide quantitative information on the forest structure which is directly related to carbon stocks. Airborne Light Detection and Ranging (A-LiDAR) is the most successful technique to retrieve three-dimensional forest structural parameters and estimate aboveground biomass (AGB) stocks (Asner et al., 2012; Longo et al., 2016; Rappaport et al., 2018) but the data are often costly to acquire and to replicate both in space and over time (Silva et al., 2017).

In addition to the spectral properties of optical remote sensing, Very High Spatial Resolution (VHSR) sensors (images with less than 5m/pixel) also acquire information on the distribution of dominant tree crowns that define the forest canopy and also canopy gaps, thereby providing important indirect indicators of forest three-dimensional structure (Meyer et al., 2018). The spatial distribution of trees, the shapes and dimensions of their crowns and the characteristics of the inter-crown gaps interact to define the forest canopy grain and can be assessed through canopy texture analysis (Couteron et al., 2005). Several studies have demonstrated the potential of texture methods to characterize VHSR canopy images (Couteron et al., 2005; Frazer et al., 2005). Among them, the FOurier-based Textural Ordination (FOTO) method has been used in a variety of tropical forests to characterize gradients of canopy grain, heterogeneity and crown size distribution (Barbier et al., 2010; Bastin et al., 2014; Couteron et al., 2005; Ploton et al., 2012; Singh et al., 2014). Case studies have shown that FOTO indices can correlate with forest structural parameters along gradients of natural variation (Couteron et al. 2005) of degradation (Ploton et al. 2012; Singh et al. 2014) or in landscapes mixing both (Bastin et al. 2014 ; Pargal et al. 2017). Lacunarity analysis, another textural approach, also captures spatial heterogeneity of forest canopies and additionally provides a quantitative measure of canopy 'gapiness' that correlates with canopy cover and gap fraction (Frazer et al., 2005; Malhi and Román-Cuesta, 2008; Ploton et al., 2017). However, the possible links between canopy texture and forest structure parameters are context dependent (Ploton et al. 2017), and relationships have to be verified and calibrated using reference data from either field plots or airborne canopy altimetry, and such data are not available in many tropical landscapes or regions. Moreover, one cannot expect the variety of stand structures generated by degradation processes to display unequivocal relationships with canopy texture variables (Rappaport et al., 2018). For instance, severe degradation may result in coarse texture (e.g. because of big gaps) as well as fine-grained aspects owing to small crowns in regenerating patches. In this sense, there is a lack in understanding and quantifying the consequences of forest degradation on canopy texture. Using unmanned aerial vehicles (UAV), the aim of this paper is to demonstrate that texture information can efficiently characterize degraded forest types. Unmanned aerial vehicles are thus a new promising tool to acquire altimetry data and very high resolution images of the canopy (Koh and Wich, 2012; Zhang et al., 2016).

Here, we used very high resolution UAV images to sample a broad range of degraded and intact forests conditions in an old deforestation pioneer front of the Brazilian Amazon. For each forest site, we combined degradation history from Landsat time series with UAV data including canopy elevation and grey-level images. Our large-area and diverse UAV coverage addressed two questions: (1) How do canopy textures correlate with forest structure parameters within a large range of degraded forest types? (2) How do disturbance type and frequency contribute to variability in texture metrics through heterogeneity, coarseness and openness canopy gradients?

In so doing, our study aims to pave the way for interpreting canopy texture in VHSR satellite images from agile UAV-based ground truthing and consequently help decision makers improve the management of degraded forests.

2. Materials and Methods

2.1. Study area

The study was carried out in the municipality of Paragominas, located in the northeastern part of the State of Pará, Brazil, and covered an area of 19,342 km² (Fig. 1). The municipality experienced different colonization processes since its foundation in 1965, which led to significant deforestation with conversion of land to pasture for cattle ranching and forest degradation through overexploitation of timber. Deforestation was accentuated by the grain agro-industry in the 2000s, dominated by intensive soybean and maize cultivation mainly in the center of the municipality (Piketty et al., 2015). We demonstrated in previous studies that the history and processes of colonization spatially differ within Paragominas (Laurent et al., 2017). This led to a mosaic of forests in very different cover states within heterogeneous landscape mosaics dominated by different land uses (Bourgoin et al., 2018; Mercier et al., 2019). In this region, forest management plans with selective logging have rarely been adopted except in CIKEL Brasil Verde Madeiras Ltda forestry company (Mazzei et al., 2010). Forest suffered from two major anthropogenic disturbances. Unplanned logging with over-logging intensity is marked by repeated frequencies over time. Fire alters deeply the understory and generate high mortality rates for canopy trees (Fig. 1)(Hasan et al., 2019; Tritsch et al., 2016).

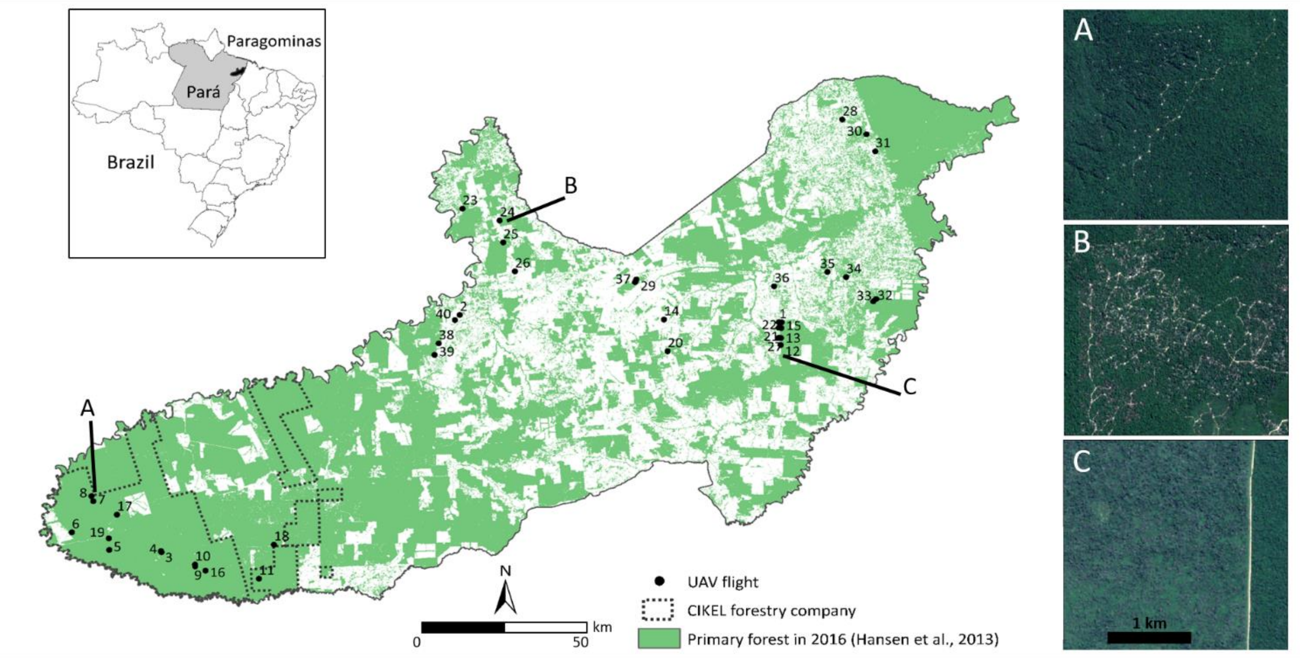

Figure 1: Location of the study site, Paragominas municipality, in Pará state in the Brazilian Amazon. Distribution of the 40 forest plots covered using UAV. Illustrations of selective logging (A), over-logging (B) and fire (C) from Google Earth® 2017

2.2. Data collection

2.2.1. UAV surveys and processing

Forty forest sites were selected in various forested landscapes to cover a large variation of disturbance types (Fig.1). Using visual interpretation from Google Earth® VHSR images validated by in-situ UAV observations, we distinguished between sites that experienced disturbances such as logging and fire and intact sites with no human-induced disturbance. We also used the management plan of the Cikel forestry company (Fig.1) that provides spatial information on undisturbed and selectively logged forests at different dates over the last 20 years.

We used a DJI mavic pro UAV carrying its original RGB camera of 12.71 megapixel resolution (DJI, Shenzhen, China). The acquisition plan was designed with Pix4D Capture software (Pix4D, Lausanne, Switzerland). We used a single grid with 80% of front and side overlap between images and a constant flight altitude of 300 meters above ground level. The objective was to maximize the overlap between each image and the total surface area mapped. As a result, the average surface mapped in each forest plot was 24 ha (~600 by 400 meters) at 10 centimeters spatial resolution (Appendix C) for a total of

739 ha. In order to generate a high quality canopy height model, each flight was constrained by several conditions:

i) Flat terrain was selected with imaged areas that overlapped with roads or agricultural fields to allow us to retrieve the ground elevation during the preprocessing step;

ii) Acquisition in the morning (9 to 11 am) and afternoon (3 to 5 pm) was preferred to avoid zenithal effects (halo and low image contrast);

iii) Either cloud free or totally cloudy sky conditions were necessary to avoid cloud shadows;

iv) Absence of wind to low wind conditions were needed to generate crisp images of the forest canopy.

Raw image data were processed to the highest density point cloud using structure from motion (SfM) followed by densification using multi-view stereo algorithms in the Pix4D software (Alonzo et al., 2018; Westoby et al., 2012). Final point cloud densities were ~27 pts.m-3 depending on the availability of viable tie points, and some other acquisition parameters (Table 1). Using the georectified point clouds, we corrected the raw images to generate RGB mosaics, which were then converted into single-band panchromatic grey level mosaics. Digital Surface Models (DSM) of the canopy (i.e. the top of the forest’s surface) at 0.10 m resolution were directly computed from the point cloud. We extracted the average ground elevation data in non-forest areas (e.g. roads, agricultural fields or canopy gaps) from the DSMs and derived canopy height models for each forest plot.

2.2.2. Landsat time series to detect forest disturbances and reconstruct degradation history

We acquired Landsat data from 1984 to 2017 (Appendix A) to detect forest disturbances along time and reconstruct degradation history for each forest site. The images at Level 1 (Tier 1 product) were pre-processed to surface reflectance by the algorithm developed by the NASA Goddard Space Flight Center (http://earthexplorer.usgs.gov/). We computed the Normalized Difference Moisture Index

(NDMI) from the Short-Wave InfraRed (SWIR) and Near InfraRed (NIR) bands as follows (Gao, 1996):

$$NDMI = NIR - SWIR/NIR + SWIR$$

This index previously used to monitor forest degradation (DeVries et al., 2015) allowed us to identify disturbance type and frequency (selective logging, over-logging and fire) at forest plot scale, using photointerpretation (Appendix B). The disturbance type was identified based on its spatial extent and shape and on the low NDMI values. Selective logging is marked by regular and spaced logging roads (Fig.1A), over-logging is marked by irregular logging roads (Fig. 1B) and fire presents open canopy structure and low values of NDMI (Silva et al., 2018; Tritsch et al., 2016). We also recorded the date of the most recent disturbance (Appendix C) which has a significant influence on the current forest structure (Rappaport et al., 2018). Figure 2 shows the diversity of forest degradation history of our sampling such as selectively logged forests, over-logged forests and over-logged and burned forests.

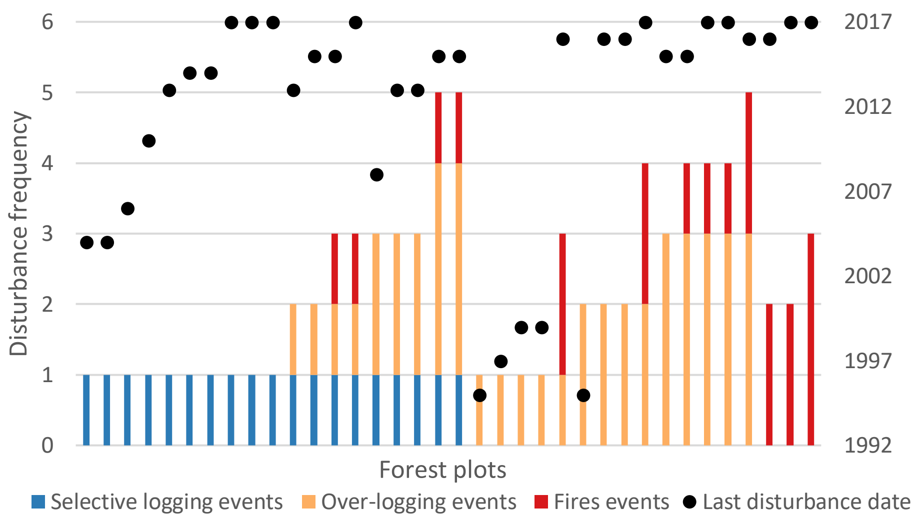

Figure 2: Forest degradation history of the 40 forest plots based on the frequency of selective logging, over-logging, fire events and date of last disturbance (4 plots are not shown as they are secondary forests).

2.3. Methods

The data analysis was based on two steps: (1) use canopy texture metrics derived from grey-level UAV images to retrieve canopy structure metrics (based on canopy height models) derived from UAV structure from motion within a large range of degraded forest types at 1 ha scale and (2) potential of canopy texture metrics to discriminate degradation history and the resulting changes in forest structures at the forest plot scale (Fig. 3).

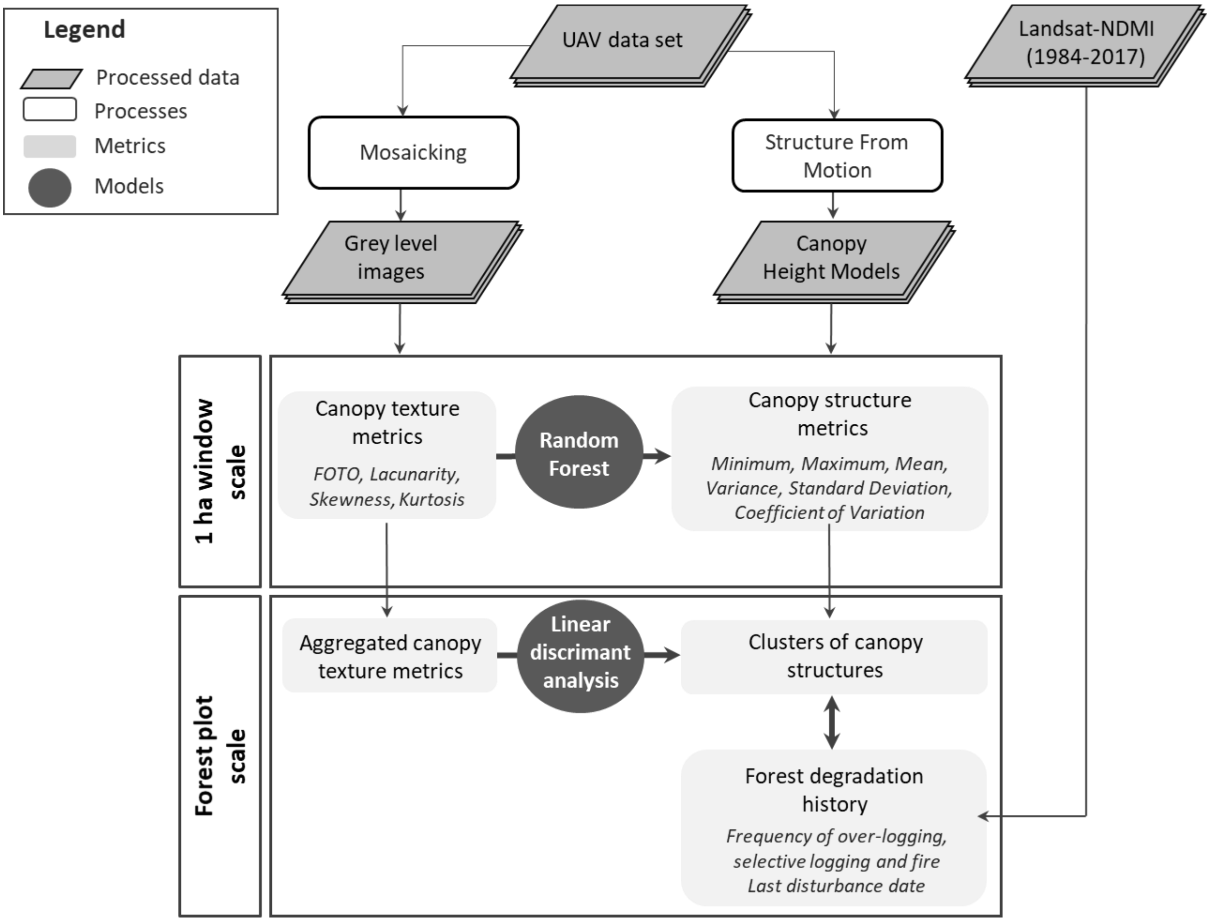

Figure 3: Workflow of the method used to evaluate the potential of canopy texture metrics to retrieve the canopy structure along the gradient of forest degradation and their relation with forest degradation history.

<u>2.3.1. Computation of forest canopy texture metrics from grey level UAV images at 1 ha scale</u>

We performed texture analysis of grey level canopy images using FOTO (Couteron, 2002) and lacunarity (Frazer et al., 2005) algorithms. We also used basic descriptors of statistical grey level distributions such as skewness and kurtosis. Each of the UAV canopy images was divided into canopy 100*100 m windows (fixed grid) for texture analysis. This size was shown in previous studies to be appropriate to capture several repetitions of the largest tree crowns (in our case 45 meters of maximum tree crown diameter) in forest stands (Ploton et al., 2017).

The FOTO method is extensively described elsewhere (Couteron, 2002; Couteron et al., 2005; Ploton et al., 2017), hence we only give here a brief outline of the procedure. When applying FOTO, each of the windows originating from the UAV images is subjected to a two-dimensional Fourier transform to enable computation of the two-dimensional periodogram. ‘Radial-’ or ‘r-spectra’ are extracted from the periodogram to provide simplified, azimuthally-averaged textural characterization. Spectra are systematically compared using the two first axes of a principal component analysis (FOTO_PCA1, FOTO_PCA2), providing an ordination along a limited number of coarseness vs. fineness gradients. In this process, windows are treated as statistical observations that are characterized and compared on the basis of their spectral profile, i.e., the way in which window grey scale variance is broken down in relation to Fourier harmonic spatial frequencies (ranging from 50 to 240 cycles/km for this study). PCA captures gradients of variation between windows spectra opposing those concentrating most variance in low frequencies (i.e. coarse textures) and those in which high frequencies retain a substantial share of variance (i.e. fine textures).

Lacunarity was defined following Frazer et al. (2005) and Malhi and Roman-Cuesta (2008). For each 100*100 m window, a moving square box of size ‘s’ was glided by one pixel at a time and the sum of all pixel spectral radiance, called the mass, was computed at each gliding position. The frequency distribution of the mass divided by the number of boxes’ positions is computed, and Lacunarity at box size ‘s’ is the squared ratio of the first and second moment of this distribution. This process was repeated for 100 box sizes ranging from 1 to 99 m and the resulting lacunarity spectrum was normalized by lacunarity at size 1. Finally, the spectra were compared using the two first axes of a PCA (Lacu_PCA1 and Lacu_PCA2 respectively), to provide an ordination of windows along inter-crown canopy openness gradients.

Routines for both FOTO (http://doi.org/10.5281/zenodo.1216005) and lacunarity methods were developed in the MatLab® environment (The MathWorks, Inc., Natick, Massachusetts, USA).

2.3.2. Computation of forest canopy structure metrics from canopy height models at 1 ha scale

From the canopy height model, six Canopy Structure Metrics (CSM) were computed in the same 100*100m window grid previously described: mean elevation (mean), minimum (min), maximum (max), variance (var), Standard Deviation (SD) and Coefficient of Variation (CV) defined as the ratio between standard deviation and mean elevation. We then compiled the six Canopy Texture Metrics, noted CTM, (FOTO_PCA1, FOTO_PCA2, Lacu_PCA1, Lacu_PCA2, Skewness, Kurtosis) and the 6 CSM.

2.3.3. Canopy texture - structure relations within a large range of degraded forest types at 1 ha scale

The ability of CTM to predict forest canopy structures was tested using regression models for each CSM based on Random Forest machine learning (RF) (Breiman, 2001).

The learning set is randomly partitioned into *k* equal size sub-samples with k=10. Each regression process is then applied where *k-1* sub samples are used as training data and the remaining ones for validation. This process is repeated by changing the training/validation sub-samples in such a way that all learning samples are used for validation. Cross-validation is a common and sound procedure in machine learning processes (Arlot and Celisse, 2010; Kohavi, 1995). The R-squared, average Root Mean Square Error (RMSE) and relative RMSE were utilized to evaluate the performance of the model. The number of trees and the number of variables used for tree nodes splitting were randomly determined using the tune function implemented in the R randomForest package, version 4.6-14 (Liaw and Wiener, 2002). The number of tree was set to 500 to reduce computation times without notable loss in accuracy.

2.3.4. Potential of canopy texture metrics to discriminate forest degradation histories at the plot scale

The forest plot scale was used to combine canopy texture and canopy structure metrics with forest degradation history. We first classified forest plots according to their canopy structures (mean CSM calculated at the plot scale) using PCA and hierarchical clustering (Ward's criterion). The number of clusters was optimized by calculating the inter-cluster variance (Ketchen Jr. and Shook, 1996). Each cluster of forest canopy structure was then related to forest degradation history by calculating the average disturbance frequency of over-logging, selective logging and fire events. We then used Linear Discriminant Analysis (LDA) to predict membership of forest structure clusters from averaged value of CTM at the plot scale. LDA algorithm tries to find a linear combination within the canopy textural metrics averaged at plot scale that maximizes separation between the barycenters of the clusters while minimizing the variation within each group of the dataset (Hamsici and Martinez, 2008; Kuhn and Johnson, 2013). We used MANOVA with Pillai's Trace tests to evaluate the significance of the multivariate inter-cluster difference computed from the 6 CTM. All processes were computed using the R packages FactoMineR (Husson et al., 2010; Lê et al., 2008) and the MASS package (Venables and Ripley, 2002).

3. Results

3.1. Forest canopy texture metrics from grey level UAV images at 1 ha scale

The two first factorial axes of the PCA accounted for 51.6% of the total variability of the r-spectra observed (Fig. 4b). FOTO_PCA1 expresses a gradient between coarse and fine texture corresponding to spatial frequencies of less than 90 cycles/km and more than 120 cycles/km, respectively (Fig. 4c). FOTO_PCA2 expresses a gradient leading from heterogeneous textures with the coexistence of low and high frequencies (negative scores) toward homogeneous intermediate frequencies in the range 90-120 cycles/km (high scores). Fine textures correspond to homogeneous distribution of small tree crowns reflecting ongoing regeneration after probable over-logging. Intermediate textures along axis 1 associate large and smaller tree crowns that characterize preserved forest with the natural distribution of high emergent trees and lower canopy trees. The left part of the scatter plot groups coarse textures corresponding to large gaps in the canopy related to logging activities. Finally, the two examples at the bottom of the plot show mixed coarse (remaining trees) and fine (low understory or shrub stratum) textures that characterize over-logged and recently burned forests.

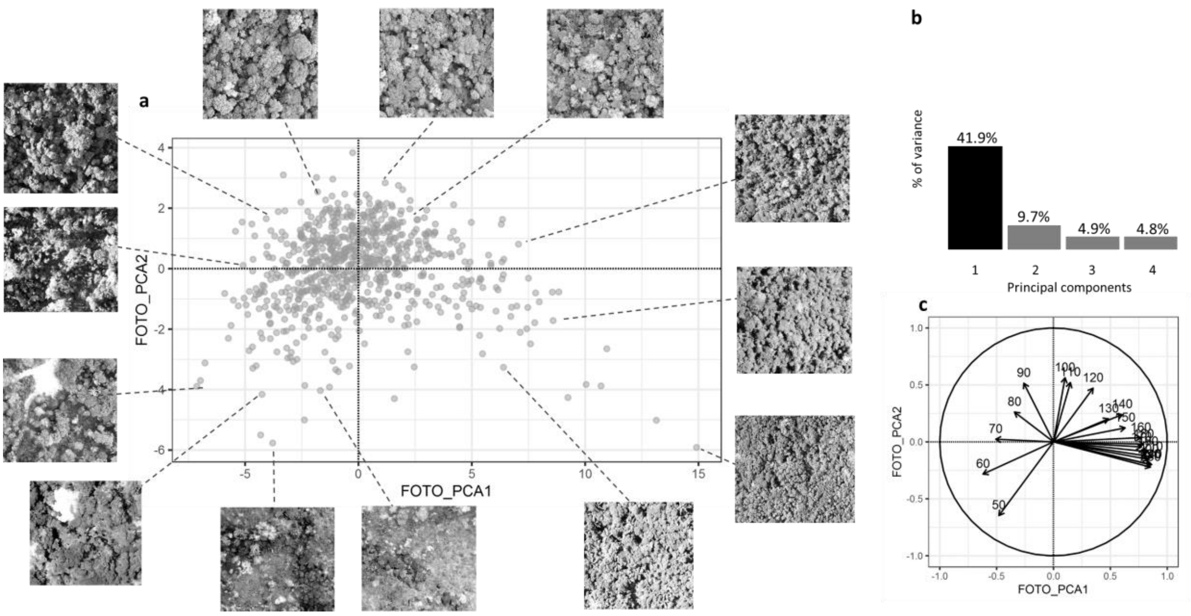

Figure 4: Canopy texture ordination based on the FOTO method applied to UAV-acquired grey level images. (a) Scatter plots of PCA scores along F1 and F2 and windows selected as illustrations. (b) Histogram of eigenvalues expressed as % of total variance. (c) Correlation circles with frequencies ranging from 50 to 240 (cycles/km).

The first factorial axe of the PCA on the lacunarity spectra account for more than 70% of total variability (Fig. 5b). Lacu_PCA1 expresses a gradient of gapiness with large gaps appearing in the extreme left part of the scatter plot (Fig. 5a) and closed canopy forest with no gaps in the extreme right part. Large gaps are tree shadows projected over large canopy gaps. Homogeneous canopies, i.e. smooth grain and a closed canopy characterizing low degradation forests were found on the positive side of the second axis (Lacu_PCA2)(11% of total variability) and vice versa for heterogeneous canopies. These are highly degraded forests (over-logged at different ages and recently burned forests) with destroyed canopies and patches of small crowns linked to the understory or to regeneration. Other axes did not reveal other structures. Substantial analogy can be observed between the main texture gradients provided by FOTO and by the lacunarity analyses.

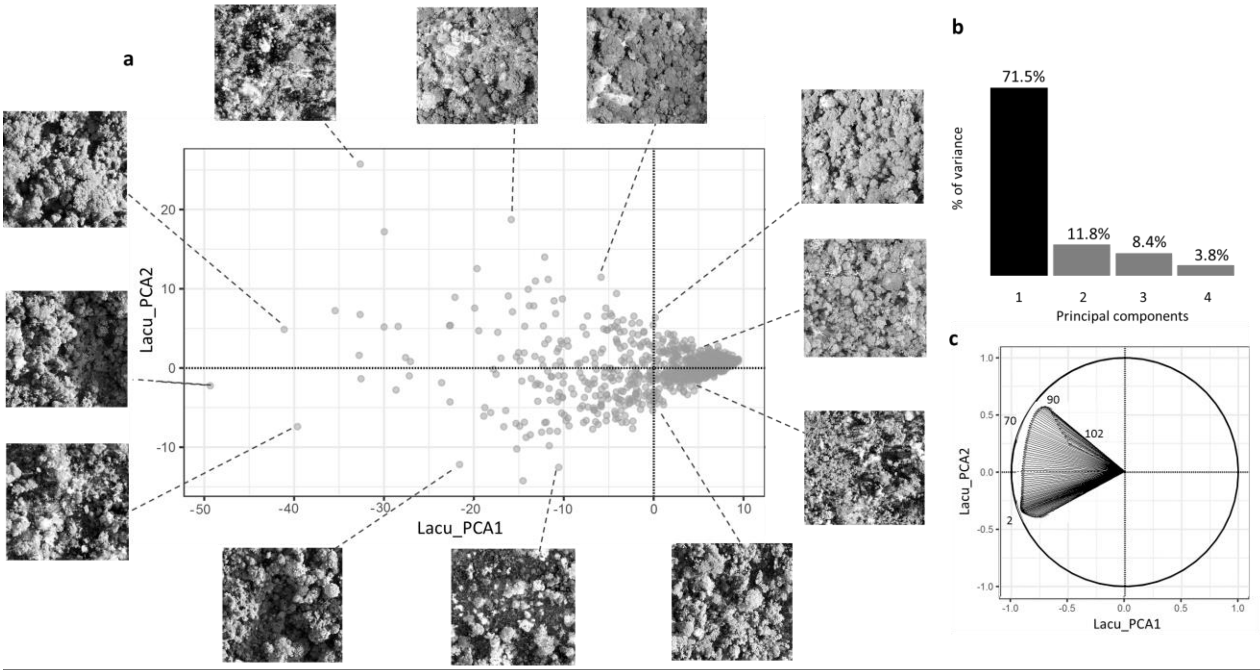

Figure 5: Canopy texture ordination based on the lacunarity method. (a) Scatter plots of PCA scores along F1 and F2 and windows selected as illustrations. (b) Histogram of eigenvalues expressed as % of total variance. (c) Correlation circles with sub-window sizes ranging from 2 to 102 pixels.

3.2. Relationships between canopy textures and forest structure parameters at 1 ha scale

The standard deviation and variance of canopy height were the CSM best explained by texture with a R^2 of 0.58 and 0.54 respectively (Table 1). These metrics pointing to the variability of canopy structure directly reflect the different processes of degradation and the associated gradients of canopy grain texture. Maximum and mean canopy height and coefficient of variation show lower relationship (resp. R^2 of 0.43, 0.38 and 0.31). The minimum height showed a low R^2 of 0.13 with CTM.

Table 1: Random forest regression models for the prediction of canopy structure metrics (CSM) from canopy texture metrics (CTM) on grey level images.

CSM	R^2	RMSE	Relative RMSE
Minimum (m)	0.13	3.49	0.94
Maximum (m)	0.43	5.66	0.76
Mean (m)	0.38	4.88	0.79
Variance	0.54	13.03	0.68

Standard deviation	0.58	1.01	0.65
Coefficient of variation	0.31	0.17	0.83

3.3. Potential of canopy texture metrics to discriminate forest degradation histories at the plot scale

3.3.1. Clusters of canopy structures and related degradation history

The clustering method allowed identifying six clusters of canopy structures (Fig. 6). **Cluster 1** groups wide open and low canopy forests with a significantly lower average canopy height (9.9 m) than the other clusters and high Standard Deviation (SD) values (6.19 m). It groups forest plots that have mainly experienced over-logging (~1.4 events) and recent fire events identified between 2015 and 2017 (1.6 in average). **Cluster 2** groups 23-year-old secondary forests characterized by a homogeneous and low canopy (average height of 13.86m and SD of 2.28). **Cluster 3** groups forest plots with homogeneous (SD of 5.10), low average canopy height (14.13m) mainly marked by over-logging (~1.5 events). **Cluster 4** has a heterogeneous canopy structure characterized by high standard deviation (SD of 7.03) which is explained by recent logging events detected in 2017 (~1.2 events) and other previous disturbances such as fire (~1 event). **Clusters 5 and 6** have similar canopy height (~22 m) but variable canopy roughness (SD ranging from 6.05 to 7.59). Their degradation histories differ as cluster 5 groups recently selectively logged forest (~0.6 events) or over-logged forests (~1 event) while cluster 6 mostly groups undisturbed forest and old selectively logged forests (more than 10 years ago). However both clusters are marked by very low (~0.1 events for cluster 5) to none fire disturbances detected. Further explanation on the different steps of the method and on the statistical results can be found in Appendix D and E.

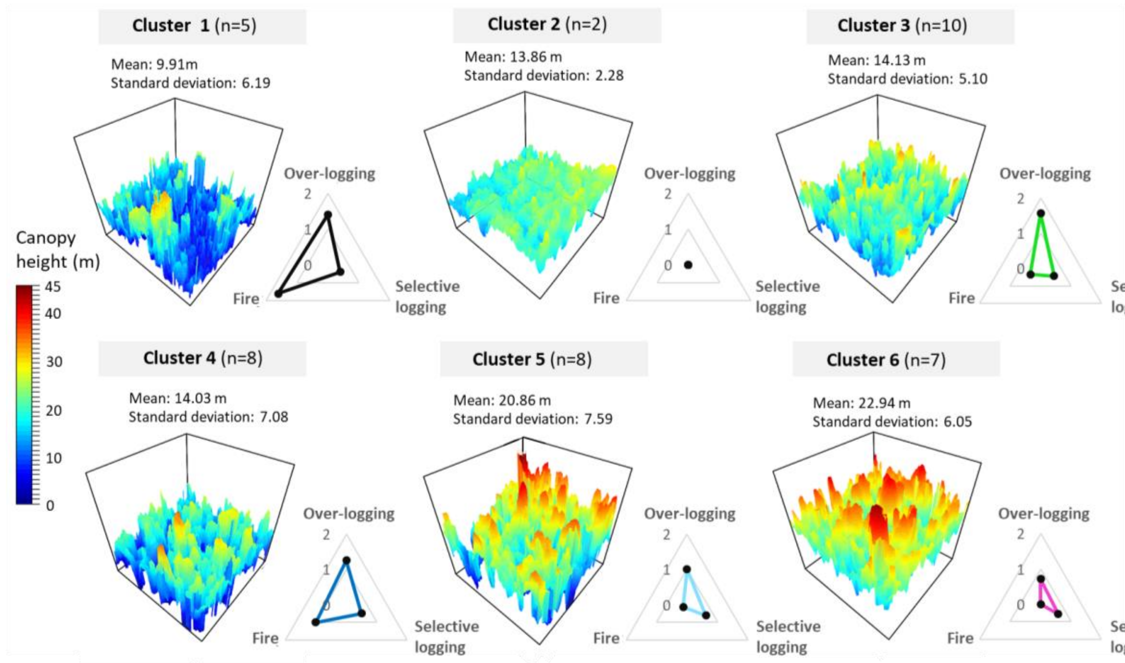

Figure 6: Three-dimensional plots of canopy height models of the 100 x 100 m windows selected to illustrate the six forest structure clusters. Radar chart shows the average frequency of over-logging, selective logging and fire disturbances detected in all forest plots within a given cluster.

3.4.2. Linear discriminant analysis at the forest plot scale

The two first discriminant components (LD1 and LD2) account for 93.6% of the total proportion of the trace i.e. the proportion of inter-cluster discrimination of the LDA based on texture (MANOVA test with p-value < 0.05)(Fig. 7a). The prominent first discriminant component is mainly correlated with FOTO_PCA1 (r=0.55 in LD1), FOTO_PCA2 (0.49 in LD1) and LACU_PCA2 (-0.79 in LD1) (Fig. 7b). The second discriminant component is mainly correlated with LACU_PCA2.

In the LD1-LD2 plane, clusters 2 and 3 are mainly separated from the rest of clusters thanks to axis LDA1. Cluster 1, 4 and 5 are discriminated along LD2. Cluster 6 has less discriminating capacity, especially compared with cluster 5.

LDA results include misclassification errors corresponding to disagreement between texture-based and structural classifications of the plots (Fig. 7a). The confusion matrix shows an overall accuracy of 55% and kappa index at 0.44 (Fig 7c). The LDA classification performed well for all clusters except cluster 6 which has the highest misclassification rate with a high rate of confusion with cluster 5. Based on CTM, clusters 5 and 6 appeared to be similar because they mainly differ in their minimum height, which logically is difficult to predict from canopy texture metrics on 2D images.

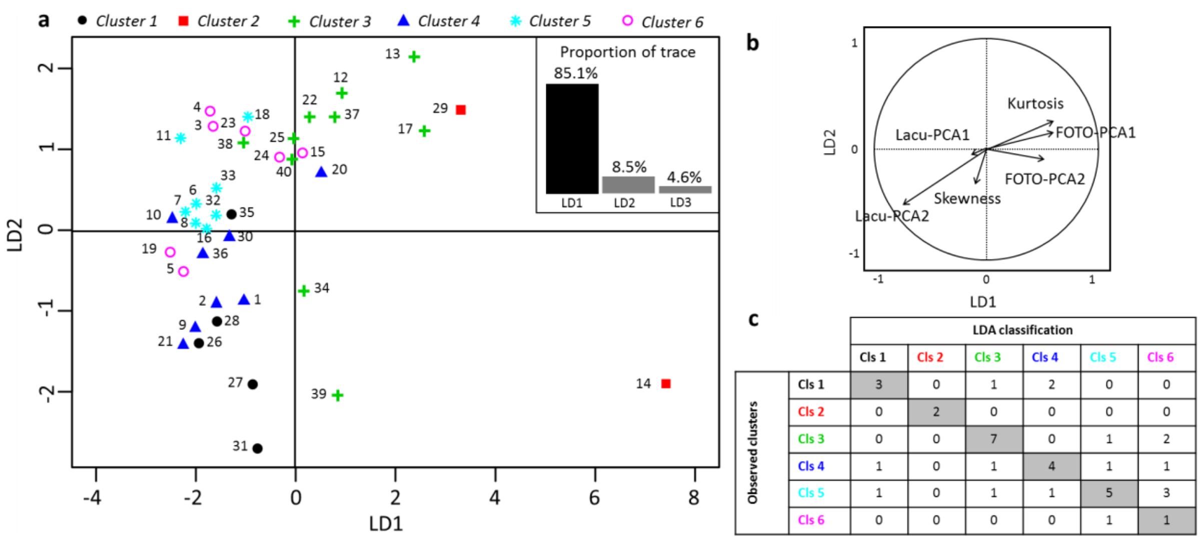

	Cls 1	Cls 2	Cls 3	Cls 4	Cls 5	Cls 6
Cls 1	3	0	1	2	0	0
Cls 2	0	2	0	0	0	0
Cls 3	0	0	7	0	1	2
Cls 4	1	0	1	4	1	1
Cls 5	1	0	1	1	5	3
Cls 6	0	0	0	0	1	1

Figure 7: (a) Scatter plot showing the distribution of the 40 forest plots with color based on the color of canopy clusters on the linear discriminant plane (LD1-2). Inset: proportions of LDA trace (b) Correlation circle of CTM with respect to the two main components (axes) of the LDA (c) Confusion matrix between observed and predicted clusters for the 40 plots (LDA classifications)

Clusters 2, 3 and 5 are distinguished along a gradient of canopy textural grain that spans from fine to coarse (FOTO-PCA1) (Fig. 8). Cluster 4 mainly presents the lowest FOTO-PCA1 and Lacunarity-PCA1 values, which correspond to the coarse texture and large gaps, respectively, typical of recent logging events. Cluster 1 has on average the coarse grain and homogeneous texture (FOTO-PCA1 and -PCA2) that characterize low vegetation strata. Finally cluster 6 (well preserved forest) has intermediate canopy grain (FOTO-PCA1 and 2) and canopy openness (Lacunarity-PCA2).

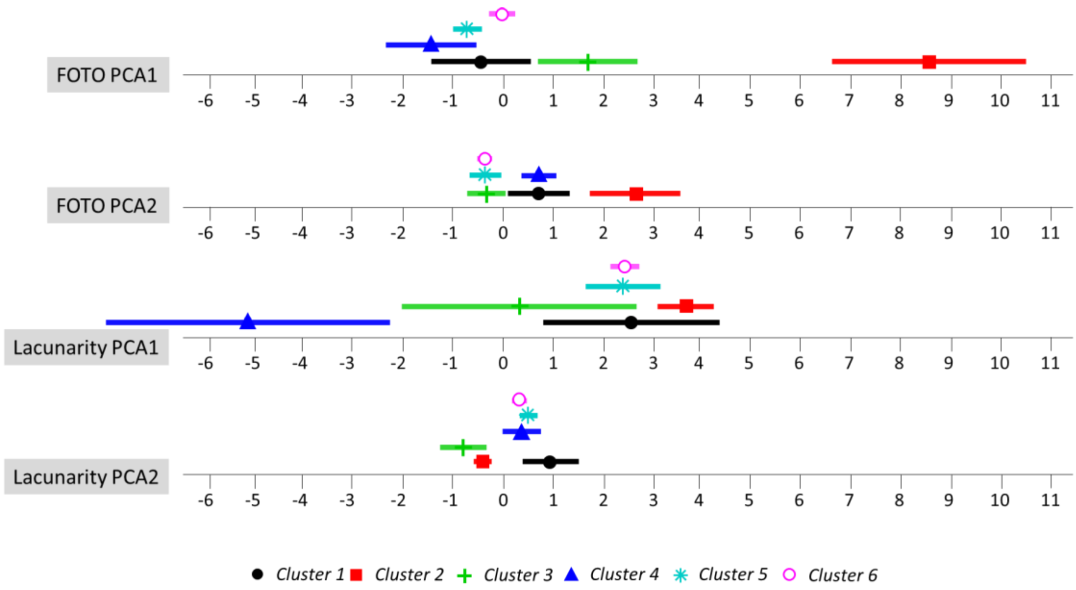

Figure 8: Mean and SD values of CTM calculated within the 6 predicted clusters using LDA.

4. Discussion

A better characterization of forest structure is crucial to tailoring forest management plans (Goldstein, 2014). In this paper, we show that canopy texture metrics extracted from very-high spatial resolution optical images acquired by unmanned aerial vehicle are clearly related to forest canopy height models and can reveal different and complex degradation history. The canopy texture metrics provide complementary information on degraded forest states compared to other remotely sensed indicators based on vegetation photosynthesis activity (Asner et al., 2009; Bullock et al., 2018; Mitchell et al., 2017). The canopy texture metrics can also be used in multidisciplinary approaches such as for the assessment of forest ecosystem services that require detailed information on forest structure (Barlow et al., 2016; Berenguer et al., 2014).

4.1. Potential of canopy texture metrics to assess degraded canopy structures

We showed that CTM can assess forest structure variability that reflects both horizontal and vertical heterogeneity induced by degradation. Through the expression of canopy grain and heterogeneity gradients, CTM provides reliable estimations of canopy roughness (standard deviation of canopy height) at 1 ha-scale. At the forest plot scale, we demonstrated the complementary of FOTO and lacunarity metrics in distinguishing between the different clusters. While FOTO and lacunarity express similar gradients of canopy texture (Figs. 4 and 5), the measure of canopy openness in lacunarity provide useful additional information to distinguish large canopy gaps from large crowns, as underlined by Ploton et al. (2017). However, the first axis of lacunarity reveals a gradient of canopy textures that could be influenced by sun-angle conditions during the UAV data acquisition. Early morning and late afternoon data acquisitions generate higher projected shadow, which drives the distribution of the data towards the negative values of the first axis. Data acquisition parameters (sun and sensor angles, clouds etc.) are known to be able to disturb grey level values and textures (Barbier and Couteron, 2015). One advantage of using UAV is that they allow better control of acquisition conditions than do satellites.

4.2. Long-term forest degradation consequences on structure explained using current canopy textures

In this study, we demonstrate the potential of single shot UAV-based canopy altimetry and texture to correlate with current structure that can reveal both past disturbances and recovery processes (Herold et al. 2011, Ghazoul and Chazdon 2017). At the forest plot scale (~24 ha), the average CSM and the variability of CSM enabled the identification of six forest clusters with specific degradation history. The link between long term degradation history and canopy structure has already been identified in previous studies that quantified carbon densities of Amazonian forests following successive logging and/or fire events (Berenguer et al., 2014; Longo et al., 2016; Rappaport et al., 2018). CTM proved to be able to differentiate between five types of degradation, although with some confusion between the less degraded forest types.

Undisturbed forests have a high closed canopy, and are homogeneous in texture with an intermediate grain associating large and medium-sized tree crowns (cluster 6). Any logging event will disrupt the canopy and create a coarse texture with greater variation in canopy height (cluster 4). Under a management plan, logging intensity is moderate (< 5 to 8 trees/ha) and the recovery time (35 years in Brazil) is expected. In that case, the coarse texture will recover and will turn back into intermediate grain (cluster 5 or 6). We showed that after seven years, the canopy texture of a logged forest resembles that of undisturbed forest (Fig. 6 and Appendix C). For unmanaged forests, subject to higher uptake, the time for the forest to recover a canopy texture of intermediate grain will be longer (e.g. plots 23 and 24). In the case of additional impacts (progressive disappearance of large crowns), the coarse canopy texture will also be maintained longer. Repetitive and intense logging have therefore triggered the complete harvesting of emergent trees, thereby weakening the capacity of forests to cope with further disturbances (Asner et al., 2002). During the recovery process, canopy is of low height and its texture is dominated by a fine and heterogeneous grain (cluster 3).

Additionally, we found that recent fire (single or multiple events) has a major impact on the damaged forest structure. The resulting highly degraded forests are characterized by coarse textures corresponding to large gaps and/or homogeneous regeneration stratum and highly damaged canopy (cluster 1). Moreover, most fires were detected in 2015, which correlated with the El Nino drought event (Berenguer et al., 2018). These findings underline the importance of the synergetic effects of logging and fire on forest structure (Dwomoh et al., 2019; Morton et al., 2013). We also found that fire was never detected (i.e. did not occur) in closed canopy and relatively low degradation forests. This confirms that heavily logged forests are more vulnerable to fire due to the presence of dead and dry vegetation resulting from logging. At a larger scale, this vulnerability is linked with the fragmentation of forest patches, which facilitates access to forest resources, accentuates dry edge effects and increases potential pressure caused by agricultural expansion (Briant et al., 2010; Broadbent et al., 2008; Silva Junior et al., 2018). The mitigation of fire occurrence through improved landscape management is therefore a priority in order to prevent further degradation and forest carbon losses (Berenguer et al., 2014).

The results of the present study reveal possible ways to address questions concerning the future management of primary degraded forests by analyzing the structure and texture of their canopy in order to better differentiate forest states and the associated degradation history. This study also opens the way for further analysis of secondary forests in abandoned lands which will certainly play a crucial role in future scenarios of landscape restoration (Chazdon et al., 2016).

4.3. UAV technology: from data acquisition to limitations and perspectives

This paper reports the first large-scale application of low cost UAV to retrieve quantitative information on closed canopy forest structures. The UAV used is inexpensive (<2,000 US$) and a highly efficient cost/time ratio was found for data acquisition in the field. In a 20 minutes flight, around 25 hectares of forest was mapped at a resolution of 10 centimeters. Other studies using UAV produced results that are comparable with LiDAR in terms of point cloud densities (Chung et al., 2019; Dandois et al., 2015) and estimations of forest structural parameters (Alonzo et al., 2018). Finally, the computation of CTM using open-source Matlab® routines is automatic and only requires the window size used for texture analysis as the user input. Window size can be adapted to forest canopy crown size and distribution, although limited variations do not alter the results much. Consequently, the workflow described here has great promise for future monitoring of tropical forest at low cost, which is interesting when airborne LiDAR is not affordable or available.

However, UAV remain limited by their inability to cover regions as large as those covered by satellite images, and climatic conditions (wind, cloud shadows) are likely to disturb the consistency of image texture and thus the automatic mapping process. Finally, regulations strongly limit the use of UAV in certain countries. Nonetheless, UAVs appears to be an efficient tool at the interface between field inventory and satellite characterization of forest structure (Koh and Wich, 2012). Unmanned aerial vehicle acquired reference data could be the basis of upscaling chains that would allow the use of spaceborne data of decreasing resolution yet increasing swath and affordability so as to reach broad scale, wall to wall mapping of forest state indicators of known accuracy.

Authors' contributions

CB, JB, LB, JO, LR, PL and VG conceived the ideas and designed methodology; CB, JB, LB and VB collected the data; CB, JB, PC, LB, HD, LR and VG analyzed the data; CB, PC, VG, LB and PS led the writing of the manuscript. All authors contributed critically to the drafts and gave final approval for publication.

Acknowledgements

This work was supported by 1) the European Union through the H2020-MSCA-RISE-2015 ODYSSEA project (Project Reference: 691053), by 2) the CNES (France) through the TOSCA CASTAFIOR project (ID 4310), by 3) the EIT through the Climate-KIC ForLand Restoration project and by 4) the CGIAR Research Program on Forest Trees and Agroforestry (FTA) and on Climate Change, Agriculture and Food Security (CCAFS), the latter with support from CGIAR Fund Donors and through bilateral funding agreements.

For details, please visit https://ccafs.cgiar.org/donors. The views expressed in this document cannot be taken to reflect the official opinions of these organizations

Conflicts of Interest: *The authors declare no conflict of interest.*

References

Alonzo, M., Andersen, H.-E., Morton, D., Cook, B., 2018. Quantifying Boreal Forest Structure and Composition Using UAV Structure from Motion. Forests 9, 119. https://doi.org/10.3390/f9030119

Arlot, S., Celisse, A., 2010. A survey of cross-validation procedures for model selection. Statist. Surv. 4, 40–79. https://doi.org/10.1214/09-SS054

Asner, G.P., Keller, M., Pereira, R., Zweede, J.C., 2002. Remote sensing of selective logging in Amazonia: Assessing limitations based on detailed field observations, Landsat ETM+, and textural analysis. Remote Sensing of Environment 80, 483–496.

Asner, G.P., Knapp, D.E., Balaji, A., Páez-Acosta, G., 2009. Automated mapping of tropical deforestation and forest degradation: CLASlite. Journal of Applied Remote Sensing 3, 033543–033543.

Asner, G.P., Mascaro, J., Muller-Landau, H.C., Vieilledent, G., Vaudry, R., Rasamoelina, M., Hall, J.S., van Breugel, M., 2012. A universal airborne LiDAR approach for tropical forest carbon mapping. Oecologia 168, 1147–1160. https://doi.org/10.1007/s00442-011-2165-z

Baccini, A., Walker, W., Carvalho, L., Farina, M., Sulla-Menashe, D., Houghton, R.A., 2017. Tropical forests are a net carbon source based on aboveground measurements of gain and loss. Science 358, 230–234. https://doi.org/10.1126/science.aam5962

Barbier, N., Couteron, P., 2015. Attenuating the bidirectional texture variation of satellite images of tropical forest canopies. Remote Sensing of Environment 171, 245–260. https://doi.org/10.1016/j.rse.2015.10.007

Barbier, N., Couteron, P., Proisy, C., Malhi, Y., Gastellu-Etchegorry, J.-P., 2010. The variation of apparent crown size and canopy heterogeneity across lowland Amazonian forests: Amazon forest canopy properties. Global Ecology and Biogeography 19, 72–84. https://doi.org/10.1111/j.1466-8238.2009.00493.x

Barlow, J., Lennox, G.D., Ferreira, J., Berenguer, E., Lees, A.C., Nally, R.M., Thomson, J.R., Ferraz, S.F. de B., Louzada, J., Oliveira, V.H.F., Parry, L., Ribeiro de Castro Solar, R., Vieira, I.C.G., Aragão, L.E.O.C., Begotti, R.A., Braga, R.F., Cardoso, T.M., Jr, R.C. de O., Souza Jr, C.M., Moura, N.G., Nunes, S.S., Siqueira, J.V., Pardini, R., Silveira, J.M., Vaz-de-Mello, F.Z., Veiga, R.C.S., Venturieri, A., Gardner, T.A., 2016. Anthropogenic disturbance in tropical forests can double biodiversity loss from deforestation. Nature 535, 144–147. https://doi.org/10.1038/nature18326

Bastin, J.-F., Barbier, N., Couteron, P., Adams, B., Shapiro, A., Bogaert, J., De Cannière, C., 2014. Aboveground biomass mapping of African forest mosaics using canopy texture analysis: toward a regional approach. Ecological applications 24, 1984–2001.

Berenguer, E., Ferreira, J., Gardner, T.A., Aragão, L.E.O.C., De Camargo, P.B., Cerri, C.E., Durigan, M., Oliveira, R.C.D., Vieira, I.C.G., Barlow, J., 2014. A large-scale field assessment of carbon stocks in human-modified tropical forests. Global Change Biology 20, 3713–3726. https://doi.org/10.1111/gcb.12627

Berenguer, E., Malhi, Y., Brando, P., Cardoso, A., Cordeiro, N., Ferreira, J., Franca, F., Rossi, L.C., 2018. Tree growth and stem carbon accumulation in human-modified Amazonian forests following drought and fire 8.

Bourgoin, C., Blanc, L., Bailly, J.-S., Cornu, G., Berenguer, E., Oszwald, J., Tritsch, I., Laurent, F., Hasan, A.F., Sist, P., Gond, V., 2018. The Potential of Multisource Remote Sensing for Mapping the Biomass of a Degraded Amazonian Forest 21.

Breiman, L., 2001. Random forests. Machine learning 45, 5–32.

Briant, G., Gond, V., Laurance, S.G.W., 2010. Habitat fragmentation and the desiccation of forest canopies: A case study from eastern Amazonia. Biological Conservation 143, 2763–2769. https://doi.org/10.1016/j.biocon.2010.07.024

Broadbent, E., Asner, G., Keller, M., Knapp, D., Oliveira, P., Silva, J., 2008. Forest fragmentation and edge effects from deforestation and selective logging in the Brazilian Amazon. Biological Conservation 141, 1745–1757. https://doi.org/10.1016/j.biocon.2008.04.024

Bullock, E.L., Woodcock, C.E., Olofsson, P., 2018. Monitoring tropical forest degradation using spectral unmixing and Landsat time series analysis. Remote Sensing of Environment. https://doi.org/10.1016/j.rse.2018.11.011

Chazdon, R.L., Brancalion, P.H.S., Laestadius, L., Bennett-Curry, A., Buckingham, K., Kumar, C., Moll-Rocek, J., Vieira, I.C.G., Wilson, S.J., 2016. When is a forest a forest? Forest concepts and definitions in the era of forest and landscape restoration. Ambio 45, 538–550. https://doi.org/10.1007/s13280-016-0772-y

Chung, C.-H., Wang, C.-H., Hsieh, H.-C., Huang, C.-Y., 2019. Comparison of forest canopy height profiles in a mountainous region of Taiwan derived from airborne lidar and unmanned aerial vehicle imagery. GIScience & Remote Sensing 56, 1289–1304. https://doi.org/10.1080/15481603.2019.1627044

Couteron, P., 2002. Quantifying change in patterned semi-arid vegetation by Fourier analysis of digitized aerial photographs. International Journal of Remote Sensing 23, 3407–3425. https://doi.org/10.1080/01431160110107699

Couteron, P., Pelissier, R., Nicolini, E.A., Paget, D., 2005. Predicting tropical forest stand structure parameters from Fourier transform of very high-resolution remotely sensed canopy images. Journal of applied ecology 42, 1121–1128.

Couteron, Pierre, Pelissier, R., Nicolini, E.A., Paget, D., 2005. Predicting tropical forest stand structure parameters from Fourier transform of very high-resolution remotely sensed canopy images: *Predicting tropical forest stand structure*. Journal of Applied Ecology 42, 1121–1128. https://doi.org/10.1111/j.1365-2664.2005.01097.x

Dandois, J., Olano, M., Ellis, E., 2015. Optimal Altitude, Overlap, and Weather Conditions for Computer Vision UAV Estimates of Forest Structure. Remote Sensing 7, 13895–13920. https://doi.org/10.3390/rs71013895

DeVries, B., Decuyper, M., Verbesselt, J., Zeileis, A., Herold, M., Joseph, S., 2015. Tracking disturbance-regrowth dynamics in tropical forests using structural change detection and Landsat time series. Remote Sensing of Environment 169, 320–334. https://doi.org/10.1016/j.rse.2015.08.020

Dwomoh, F.K., Wimberly, M.C., Cochrane, M.A., Numata, I., 2019. Forest degradation promotes fire during drought in moist tropical forests of Ghana. Forest Ecology and Management 440, 158–168. https://doi.org/10.1016/j.foreco.2019.03.014

Frazer, G.W., Wulder, M.A., Niemann, K.O., 2005. Simulation and quantification of the fine-scale spatial pattern and heterogeneity of forest canopy structure: A lacunarity-based method designed for analysis of continuous canopy heights. Forest Ecology and Management 214, 65–90. https://doi.org/10.1016/j.foreco.2005.03.056

Frolking, S., Palace, M.W., Clark, D.B., Chambers, J.Q., Shugart, H.H., Hurtt, G.C., 2009. Forest disturbance and recovery: A general review in the context of spaceborne remote sensing of impacts on aboveground biomass and canopy structure. Journal of Geophysical Research 114. https://doi.org/10.1029/2008JG000911

Gao, B., 1996. NDWI—A normalized difference water index for remote sensing of vegetation liquid water from space. Remote Sensing of Environment 58, 257–266. https://doi.org/10.1016/S0034-4257(96)00067-3

Ghazoul, J., Chazdon, R., 2017. Degradation and Recovery in Changing Forest Landscapes: A Multiscale Conceptual Framework. Annual Review of Environment and Resources 42, 161–188.

Goetz, S., Hansen, M., Houghton, R.A., Walker, W., Laporte, N.T., Busch, J., 2014. Measurement and Monitoring for REDD+: The Needs, Current Technological Capabilities, and Future Potential. SSRN Electronic Journal. https://doi.org/10.2139/ssrn.2623076

Goldstein, J.E., 2014. The Afterlives of Degraded Tropical Forests: New Value for Conservation and Development. Environment and Society: Advances in Research 5, 124–140. https://doi.org/10.3167/ares.2014.050108

Hamsici, O.C., Martinez, A.M., 2008. Bayes Optimality in Linear Discriminant Analysis. IEEE Transactions on Pattern Analysis and Machine Intelligence 30, 647–657. https://doi.org/10.1109/TPAMI.2007.70717

Hasan, A.F., Laurent, F., Messner, F., Bourgoin, C., Blanc, L., 2019. Cumulative disturbances to assess forest degradation using spectral unmixing in the north-eastern Amazon. Appl Veg Sci avsc.12441. https://doi.org/10.1111/avsc.12441

Herold, M., Román-Cuesta, R.M., Mollicone, D., Hirata, Y., Van Laake, P., Asner, G.P., Souza, C., Skutsch, M., Avitabile, V., MacDicken, K., 2011. Options for monitoring and estimating historical carbon emissions from forest degradation in the context of REDD+. Carbon balance and management 6, 13.

Hirschmugl, M., Gallaun, H., Dees, M., Datta, P., Deutscher, J., Koutsias, N., Schardt, M., 2017. Methods for mapping forest disturbance and degradation from optical earth observation data: A review. Current Forestry Reports 3, 32–45.

Husson, F., Josse, J., Pages, J., 2010. Principal component methods - hierarchical clustering - partitional clustering: why would we need to choose for visualizing data? 17.

Ketchen Jr., D.J., Shook, C.L., 1996. The Application Of Cluster Analysis In Strategic Management Research: An Analysis And Critique. Strategic Management Journal 17, 441–458. https://doi.org/10.1002/(SICI)1097-0266(199606)17:6<441::AID-SMJ819>3.0.CO;2-G

Koh, L.P., Wich, S.A., 2012. Dawn of Drone Ecology: Low-Cost Autonomous Aerial Vehicles for Conservation. Tropical Conservation Science 5, 121–132. https://doi.org/10.1177/194008291200500202

Kohavi, R., 1995. A Study of Cross-Validation and Bootstrap for Accuracy Estimation and Model Selection 7.

Kuhn, M., Johnson, K., 2013. Applied predictive modeling. Springer, New York.

Laurent, F., Arvor, D., Daugeard, M., Osis, R., Tritsch, I., Coudel, E., Piketty, M.-G., Piraux, M., Viana, C., Dubreuil, V., Hasan, A.F., Messner, F., 2017. Le tournant environnemental en Amazonie : ampleur et limites du découplage entre production et déforestation. EchoGéo. https://doi.org/10.4000/echogeo.15035

Lê, S., Josse, J., Husson, F., 2008. FactoMineR : An R Package for Multivariate Analysis. Journal of Statistical Software 25. https://doi.org/10.18637/jss.v025.i01

Lewis, S.L., Edwards, D.P., Galbraith, D., 2015. Increasing human dominance of tropical forests. Science 349, 827–832. https://doi.org/10.1126/science.aaa9932

Liaw, A., Wiener, M., 2002. Classification and regression by randomForest. R news 2, 18–22.

Longo, M., Keller, M., dos-Santos, M.N., Leitold, V., Pinagé, E.R., Baccini, A., Saatchi, S., Nogueira, E.M., Batistella, M., Morton, D.C., 2016. Aboveground biomass variability across intact and degraded forests in the Brazilian Amazon: AMAZON INTACT AND DEGRADED FOREST BIOMASS. Global Biogeochemical Cycles 30, 1639–1660. https://doi.org/10.1002/2016GB005465

Malhi, Y., Gardner, T.A., Goldsmith, G.R., Silman, M.R., Zelazowski, P., 2014. Tropical Forests in the Anthropocene. Annual Review of Environment and Resources 39, 125–159. https://doi.org/10.1146/annurev-environ-030713-155141

Malhi, Y., Román-Cuesta, R.M., 2008. Analysis of lacunarity and scales of spatial homogeneity in IKONOS images of Amazonian tropical forest canopies. Remote Sensing of Environment 112, 2074–2087. https://doi.org/10.1016/j.rse.2008.01.009

Mazzei, L., Sist, P., Ruschel, A., Putz, F.E., Marco, P., Pena, W., Ferreira, J.E.R., 2010. Above-ground biomass dynamics after reduced-impact logging in the Eastern Amazon. Forest Ecology and Management 259, 367–373. https://doi.org/10.1016/j.foreco.2009.10.031

Mercier, A., Betbeder, J., Rumiano, F., Gond, V., Blanc, L., Bourgoin, C., Cornu, G., Poccard-Chapuis, R., Baudry, J., Hubert-Moy, L., 2019. Evaluation of Sentinel-1 and 2 Time Series for Land Cover Classification of Forest–Agriculture Mosaics in Temperate and Tropical Landscapes 20.

Meyer, V., Saatchi, S., Clark, D.B., Keller, M., Vincent, G., Ferraz, A., Espírito-Santo, F., d'Oliveira, M.V.N., Kaki, D., Chave, J., 2018. Canopy area of large trees explains aboveground biomass variations across neotropical forest landscapes. Biogeosciences 15, 3377–3390. https://doi.org/10.5194/bg-15-3377-2018

Mitchell, A.L., Rosenqvist, A., Mora, B., 2017. Current remote sensing approaches to monitoring forest degradation in support of countries measurement, reporting and verification (MRV) systems for REDD+. Carbon Balance and Management 12. https://doi.org/10.1186/s13021-017-0078-9

Morton, D.C., Le Page, Y., DeFries, R., Collatz, G.J., Hurtt, G.C., 2013. Understorey fire frequency and the fate of burned forests in southern Amazonia. Philosophical Transactions of the Royal Society B: Biological Sciences 368, 20120163–20120163. https://doi.org/10.1098/rstb.2012.0163

Panagiotidis, D., Abdollahnejad, A., Surový, P., Chiteculo, V., 2017. Determining tree height and crown diameter from high-resolution UAV imagery. International Journal of Remote Sensing 38, 2392–2410. https://doi.org/10.1080/01431161.2016.1264028

Ploton, P., Barbier, N., Couteron, P., Antin, C.M., Ayyappan, N., Balachandran, N., Barathan, N., Bastin, J.-F., Chuyong, G., Dauby, G., Droissart, V., Gastellu-Etchegorry, J.-P., Kamdem, N.G., Kenfack, D., Libalah, M., Mofack, G., Momo, S.T., Pargal, S., Petronelli, P., Proisy, C., Réjou-Méchain, M., Sonké, B., Texier, N., Thomas, D., Verley, P., Zebaze Dongmo, D., Berger, U., Pélissier, R., 2017. Toward a general tropical forest biomass prediction model from very high resolution optical satellite images. Remote Sensing of Environment 200, 140–153. https://doi.org/10.1016/j.rse.2017.08.001

Ploton, P., Pélissier, R., Proisy, C., Flavenot, T., Barbier, N., Rai, S.N., Couteron, P., 2012. Assessing aboveground tropical forest biomass using Google Earth canopy images. Ecological Applications 22, 993–1003.

Potapov, P., Hansen, M.C., Laestadius, L., Turubanova, S., Yaroshenko, A., Thies, C., Smith, W., Zhuravleva, I., Komarova, A., Minnemeyer, S., others, 2017. The last frontiers of wilderness: Tracking loss of intact forest landscapes from 2000 to 2013. Science Advances 3, e1600821.

Putz, F.E., Redford, K.H., 2010. The Importance of Defining ‘Forest’: Tropical Forest Degradation, Deforestation, Long-term Phase Shifts, and Further Transitions: Importance of Defining ‘Forest.’ Biotropica 42, 10–20. https://doi.org/10.1111/j.1744-7429.2009.00567.x

Rappaport, D.I., Morton, D.C., Longo, M., Keller, M., Dubayah, R., Nara dos-Santos, M., 2018. Quantifying long-term changes in carbon stocks and forest structure from Amazon forest degradation. Environmental Research Letters. https://doi.org/10.1088/1748-9326/aac331

Silva, C., Hudak, A., Vierling, L., Klauberg, C., Garcia, M., Ferraz, A., Keller, M., Eitel, J., Saatchi, S., 2017. Impacts of Airborne Lidar Pulse Density on Estimating Biomass Stocks and Changes in a Selectively Logged Tropical Forest. Remote Sensing 9, 1068. https://doi.org/10.3390/rs9101068

Silva, S.S. da, Fearnside, P.M., Graça, P.M.L. de A., Brown, I.F., Alencar, A., Melo, A.W.F. de, 2018. Dynamics of forest fires in the southwestern Amazon. Forest Ecology and Management 424, 312–322. https://doi.org/10.1016/j.foreco.2018.04.041

Silva Junior, C., Aragão, L., Fonseca, M., Almeida, C., Vedovato, L., Anderson, L., 2018. Deforestation-Induced Fragmentation Increases Forest Fire Occurrence in Central Brazilian Amazonia. Forests 9, 305. https://doi.org/10.3390/f9060305

Singh, M., Malhi, Y., Bhagwat, S., 2014. Biomass estimation of mixed forest landscape using a Fourier transform texture-based approach on very-high-resolution optical satellite imagery. International Journal of Remote Sensing 35, 3331–3349. https://doi.org/10.1080/01431161.2014.903441

Souza, Jr, C., Siqueira, J., Sales, M., Fonseca, A., Ribeiro, J., Numata, I., Cochrane, M., Barber, C., Roberts, D., Barlow, J., 2013. Ten-Year Landsat Classification of Deforestation and Forest Degradation in the Brazilian Amazon. Remote Sensing 5, 5493–5513. https://doi.org/10.3390/rs5115493

Thompson, I., Mackey, B., McNulty, S., Mosseler, A., Secretariat of the convention on the biological diversity, 2009. Forest resilience, biodiversity, and climate change: a synthesis of the biodiversity, resilience, stabiblity relationship in forest ecosystems.

Tritsch, I., Sist, P., Narvaes, I., Mazzei, L., Blanc, L., Bourgoin, C., Cornu, G., Gond, V., 2016. Multiple Patterns of Forest Disturbance and Logging Shape Forest Landscapes in Paragominas, Brazil. Forests 7, 315. https://doi.org/10.3390/f7120315

Venables, W.N., Ripley, B.D., 2002. Modern Applied Statistics with S 504.

Westoby, M.J., Brasington, J., Glasser, N.F., Hambrey, M.J., Reynolds, J.M., 2012. ‘Structure-from-Motion’ photogrammetry: A low-cost, effective tool for geoscience applications. Geomorphology 179, 300–314. https://doi.org/10.1016/j.geomorph.2012.08.021

Zhang, J., Hu, J., Lian, J., Fan, Z., Ouyang, X., Ye, W., 2016. Seeing the forest from drones: Testing the potential of lightweight drones as a tool for long-term forest monitoring. Biological Conservation 198, 60–69. https://doi.org/10.1016/j.biocon.2016.03.027